JOURNAL OF CATALYSIS 77, 208–220 (1982)

Surface Composition of Promoted Iron Catalysts

D. C. SILVERMAN[1] AND M. BOUDART[2]

Department of Chemical Engineering, Stanford University, Stanford, California 94305

Received December 29, 1981; revised May 10, 1982

Auger electron spectroscopy (AES) has been used to estimate the surface composition of promoted iron catalysts for ammonia synthesis. An equation was developed from which the surface concentrations of iron and promoter are calculated from the Auger current. The equation validity as an estimation tool is verified by the agreement between the calculated iron surface mole fraction and the iron area fraction determined by the reliable technique of CO chemisorption. On doubly (K_2O–Al_2O_3) promoted catalysts, the K_2O mole fraction determined by AES agrees with the area fraction determined by CO_2 chemisorption. On multiply (CaO–K_2O–Al_2O_3) promoted catalysts CO_2 chemisorption is not applicable. AES results show that most of the surface is covered with CaO and K_2O. A surface model is proposed for the doubly promoted catalyst. The promoter is believed to be present in surface islands, approximately 2 nm in diameter and less than 1 nm in thickness, an area of pure iron between them. Within the island, the Al^{3+} is proposed to lie below the K_2O, thus being screened from the surface.

INTRODUCTION

Iron catalysts are used for the ammonia synthesis from dinitrogen and dihydrogen and for Fischer–Tropsch synthesis. These catalysts are made by fusing Fe_3O_4 with small amounts (1 to 10% by weight) of oxide promoters (Al_2O_3, K_2O, CaO). Prior to use, the iron portion of the catalyst is reduced in either dihydrogen or synthesis gas.

The surface composition traditionally has been determined by the technique of selective chemisorption of CO and CO_2 and the physisorption of N_2, all at low temperatures (*1–3*). Molecules of CO and CO_2 are assumed to chemisorb on iron and K_2O respectively in a nondissociative fashion. Neither molecule is assumed to chemisorb on "free" Al_2O_3. The area occupied by each molecule is estimated and a quantitative estimate of the fraction of each component at the surface is obtained by comparing the amount of each chemisorbed gas with the amount of physisorbed dinitrogen at monolayer coverage. The technique was originally applied to unpromoted, singly (Al_2O_3) promoted, and doubly (Al_2O_3–K_2O) promoted iron catalysts. The results indicate that a large portion of the surface is covered with promoters.

The area occupied by chemisorbed CO when divided by the area occupied by physisorbed dinitrogen at monolayer coverage determines the iron area fraction. This conclusion is substantiated by studies on unpromoted and singly (Al_2O_3) promoted iron catalysts (*2, 4*). In the latter case, alumina area fraction was obtained from exchange between surface oxygen and gas-phase $H_2{}^{18}O$. One small limitation was found. Uptake of CO by iron was found to be greater at 195 K than at 90 K (*2*). Therefore, the "best" area of a CO molecule to be used to calculate the iron area fraction is slightly dependent on the temperature at which the CO chemisorption is performed.

To calculate this surface iron mole fraction from the area fraction determined by CO chemisorption, several assumptions must be made. All models of CO chemisorption have assumed that one CO mole-

[1] Present address: Monsanto Company, St. Louis, Mo. 63167.

[2] To whom queries should be sent.

0021-9517/82/090208-13$02.00/0

cule could potentially chemisorb on each surface iron atom (*2, 5*). This picture is consistent with the fact that the iron–carbon bond is linear and not bridged. (*6*). The iron surface is nonuniform in that planes of various orientations are exposed (*2*). However, there is an abundance of LEED evidence that shows that CO can chemisorb on a number of metallic planes in a hexagonal, close-packed structure out of registry with the surface metal atoms (*7*). If this nonregistry occurs on iron under selective chemisorption conditions, the assumed stoichiometry would be slightly affected. From the distance between the surface iron atoms on low-index planes and from the size of a CO molecule, an average stoichiometry of CO to surface Fe on the nonuniform iron surface can be determined. The best estimate of this stoichiometry is one CO to about two surface + subsurface Fe, where subsurface iron denotes iron atoms on open planes which, though exposed, are hindered from chemisorbing CO by the iron atoms above (*8*).

Though CO appears to be an adequate probe for iron, CO_2 may be nonselective in that it chemisorbs on $(n,\gamma)Al_2O_3$ (which may not be of the same structure as it is on the catalyst surface), and CO_2 has been shown to be capable of adsorbing on evaporated iron films (*9–11*). Besides, CO_2 cannot distinguish between two basic promoters such as CaO and K_2O. Finally, neither CO_2 nor CO can detect possible surface impurities such as sulfur.

The above ambiguities make reexamination of the surface composition of promoted iron catalysts highly desirable. For this purpose Auger electron spectroscopy (AES), an independent, direct technique which has been reviewed elsewhere (*12, 13*), has been employed. Many of the reported AES studies have dealt with either single crystals or polycrystalline foils or films of one or two main components with impurities removed by argon ion bombardment. Quantitative analysis by AES has always required some type of calibrations by overlayers of pure components or a reference standard of the material of interest. In our case, prior calibration was not feasible. Surface roughness of the catalyst would have been impossible to duplicate in a reference standard. In addition, the catalyst surface could not be cleaned by argon iron bombardment. It would have removed what was to be determined. An alternate method was adopted.

The approach taken to adapt AES to this problem was threefold. First, an equation was developed to calculate surface composition from the Auger current. This equation used actual physical parameters as either reported in the literature or as estimated to obtain a surface composition from the Auger current without calibration with a reference standard. Second, an *in situ* reduction scheme was developed and tested through the use of an iron foil as a standard. Third, the equation and reduction scheme were applied to a doubly (Al_2O_3–K_2O) promoted iron catalyst. Since CO chemisorption provides reliable values for iron area fraction, the validity of the AES equation for estimation would be supported by agreement between the two values for iron from chemisorption and AES respectively. Then, surface amounts of K_2O as determined by AES could be used to examine the validity of CO_2 chemisorption. Then AES could be used to examine a singly (Al_2O_3) and a multiply (Al_2O_3–K_2O–CaO) promoted iron catalyst. In the latter case, CO_2 chemisorption would be ambiguous because of the two basic promoters.

EXPERIMENTAL

AES

The spectra were taken in an ultrahigh-vacuum (UHV) chamber modified for AES (*14*). An electron beam of 2.0-keV energy was used to excite the Auger transitions at about 15 to 20° with respect to the surface to obtain maximum sensitivity. All samples were resistively heated and the heating was timed for approximately 90 to 95% on and 5 to 10% off over a 300-s period so that the

chamber would not become excessively warm. A fan kept air circulating over the outside of the chamber as well. Energy analysis of the emitted electrons was done by a 4 gridded, retarding field analyzer. All spectra were recorded in the second derivative mode to reduce the background caused by secondary electrons.

Catalyst Samples

The doubly promoted iron catalyst from the Fixed Nitrogen Research Laboratory was obtained from Professor J. Gryder at Johns Hopkins University. This catalyst was No. 441 (0.85 wt% Al_2O_3–0.27 wt% K_2O). The singly promoted catalyst, also from the Fixed Nitrogen Research Laboratory and obtained from Professor J. Gryder, was No. 954 (10.2 wt% Al_2O_3). The multiply promoted catalyst, KM1, was obtained from Haldor Topsøe. It had a promoter concentration of 3 wt% Al_2O_3, 3 wt% CaO, and 0.75 wt% K_2O.

Reduction Procedure

The doubly and multiply promoted catalysts (about 10^{-3} kg) were initially prereduced at approximately 700 K for 48 h in flowing H_2 in a separate apparatus (*15*), and then passivated for transfer to the UHV chamber. Passivation for this catalyst was performed at room temperature. Passivation took five steps. First, helium (99.995% purity) was flowed over a molecular sieve at 78 K and then over the sample for approximately 1 h to eliminate dihydrogen from the Pyrex cell. Then, three successive room-temperature O_2 treatments were performed by adding O_2 to the gas manifold and by pushing it through the cell with helium for about 1500 s at dioxygen pressures ca. 1, 6.5×10^2, and 5×10^3 Pa, respectively. Then, air was allowed to diffuse back into the cell. Finally, the sample was unloaded.

The prereduction condition for the singly promoted catalyst had to be altered because of the difficulty in passivating only the outer layers. The passivation as described above had to be done at 78 K. This catalyst absorbed so much oxygen during room passivation that it could not be rereduced in the UHV chamber.

After unloading these passivated samples, they were mounted in the UHV chamber as follows. A Pt/Pt138h thermocouple was spot-welded to a 1.3×10^{-4}-m molybdenum screen and the entire screen and thermocouple were degreased by immersion in toluene and then methanol. A small amount of prereduced catalyst was placed onto the screen and a small drop of distilled water was added. The sample and screen were then pressed between two stainless-steel plates on a Carver Laboratory Press at 6.0×10^7 Pa overnight. The sample was then mounted in the UHV chamber.

After mounting, the prereduced and passivated doubly and multiply promoted catalysts were treated in the following manner in the UHV chamber. Upon pumpdown, the sample was held at 500 to 600 K for approximately 3 h while pumping in order to eliminate chemisorbed gases from the surface. A spectrum was taken before and after this step. Then an initial reduction in H_2 at 560 to 1330 Pa was performed for 5 to 6 h at 800 to 900 K. A spectrum was taken at this time when the dihydrogen background reached 10^{-3} Pa. The chamber was then baked out and a base pressure of 6.5×10^{-8} Pa was achieved. Another reduction was performed at about 100 Pa for 5 to 6 h at the same temperature and spectra were taken immediately after 10^{-3} Pa was reached and then when 2×10^{-7} Pa was achieved. A short cleaning in 10^{-4} Pa H_2 was performed at this lower pressure, but it was not needed. Both results were identical within experimental error.

The *in situ* reduction procedure for the singly promoted catalyst again had to be changed because of the difficulty in reducing this sample. This difficulty is probably a reflection of its larger surface area (*2*). The fact that the singly promoted catalyst has a surface area of 1×10^4 to 1.5×10^4 $m^2\ kg^{-1}$

(*5*) means that at least 1 to 10 Pa (based on the size of the UHV chamber) of water vapor could be present if all of the oxygen, five to ten monolayers (*2*), absorbed during passivation reacted during one reduction cycle. To completely remove bulk and surface oxide from multiply promoted catalysts, P_{H_2O}/P_{H_2} ratios of less than 5×10^{-4} have been found (*17*) to be necessary at normal reduction temperatures. For this reason, successive reductions in approximately 1.8×10^3 Pa dihydrogen were performed at 900 to 1000 K. The temperature was increased to make the equilibrium more favorable. This increased reduction temperature will tend to decrease the catalyst surface area. However, the relative concentration of iron and promoter should remain almost unchanged with this increased temperature. This constancy was verified in the case of a promoted ($MgO–K_2O$) iron Fischer–Tropsch catalyst subjected to various reduction temperatures (*18*).

The UHV chamber was not baked out for this catalyst. This normal UHV procedure caused very extensive reoxidation of the catalyst. After such a bakeout, rereduction of the catalyst became extremely difficult, if not impossible, because of the unfavorable equilibrium. Lack of bakeout means that the surface of this catalyst might not remain completely clean during the recording of an entire spectrum. To try to overcome this problem, spectra of this catalyst were taken in a large (~1.0 Pa) dihydrogen atmosphere.

Selective Chemisorption

Surface composition of the doubly promoted catalyst was determined by means of selective chemisorption as well. A sample ($\cong 10^{-3}$ kg) was placed into a Pyrex reactor and was reduced in flowing dihydrogen (volumetric flow rate $\cong 10^{-6}$ m^3 s^{-1}) that was purified by diffusion through a Pd/Ag thimble. The catalyst temperature was maintained at 720 K and the reduction time was approximately 60 h. After this 60 h, the catalyst was pumped for 3 h at about 1.3×10^{-3} Pa and 720 K to remove chemisorbed dihydrogen. The sample was then cooled while pumping, and when the reactor reached room temperature, the catalyst was isolated from the vacuum system.

The chemisorption experiments were performed on a conventional volumetric adsorption apparatus with a mercury manometer and gas burette. Selective chemisorption of CO at 195 K, CO_2 at 195 K, and physisorption of N_2 at 78 K were used to determine the amount of surface Fe and K_2O as well as the BET monolayer coverage, respectively.

Gas Purification

The H_2 used in the UHV chamber and in the auxiliary apparatus for reduction and chemisorption was purified by diffusion through a Pd/Ag thimble. The O_2 used in passivation was research grade from Matheson Corporation and had been passed over a molecular sieve trap at 195 K. The CO, CO_2, and N_2 used in the selective chemisorption study were purified by passage over molecular sieves at 195, 195, and 78 K, respectively.

RESULTS

Qualitative AES

The experimental conditions were capable of reducing an iron foil (2.54×10^{-5} m thick, 99.999% nominal purity) in that no oxygen was detected on the surface after postbakeout reduction (*8*). None could be brought to the surface by heating or by allowing the sample to stand under vacuum. Most of the carbon impurity, but none of the submonolayer sulfur impurity, was removed. The conditions chosen for reduction were adequate. The catalysts can be considered to be reduced.

For the AES spectra, the peak assignments are listed in Table 1. X-Ray levels are used. As is customary, the energy corresponds to the minimum in the second derivative spectra.

TABLE 1

AES Peak Assignments

Element	Transition	Energy (eV)
C	$KL_{23}L_{23}$	272
O	KL_1L_1	470
O	KL_1L_{23}	485
O	$KL_{23}L_{23}$	508
$Al(Al_2O_3)$	$L_{23}V_0V_0$	54
S	$L_{23}M_1M_{23}$	139
S	$L_{23}M_{23}M_{23}$	149
K	$L_{23}M_1M_1$	218
K	$L_{23}M_1M_{23}$	232
K	$L_{23}M_{23}M_{23}$	249
K	$L_{23}M_{23}N_1$	272
Fe	$M_{23}VV$	47
Fe	M_1VV	82
Fe	$L_3M_1M_{23}$	565
Fe	$L_2M_1M_{23}$	580
Fe	$L_{23}M_{23}M_{23}$	595

Note. All peaks except $Al(Al_2O_3)$ are from Ref. (*32*). $Al(Al_2O_3)$ is from Ref. (*18*).

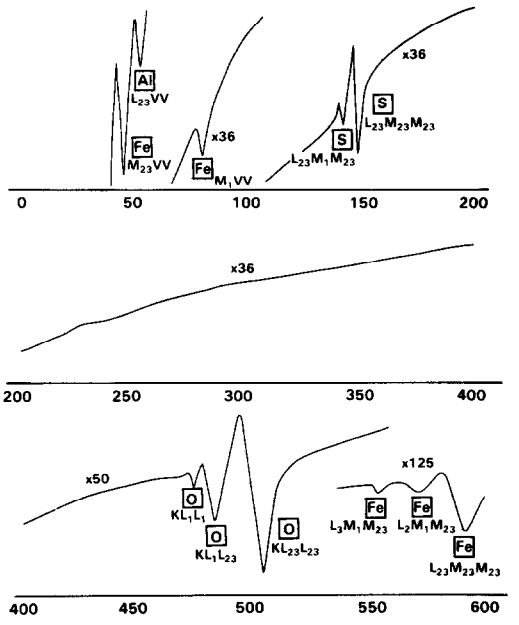

FIG. 2. AES spectrum (second derivative mode) of a completely reduced singly promoted iron catalyst. Scale in electron volts.

Shown in Figs. 1–3 are the spectra of the fully reduced samples. The 42- and 50-eV oxidized iron doublets visible on oxidized samples have merged into the 47-eV metallic iron peak. The aluminum 54-eV $L_{23,Al}\,V_0V_0$ peak, which might correspond to a cross transition between aluminum and

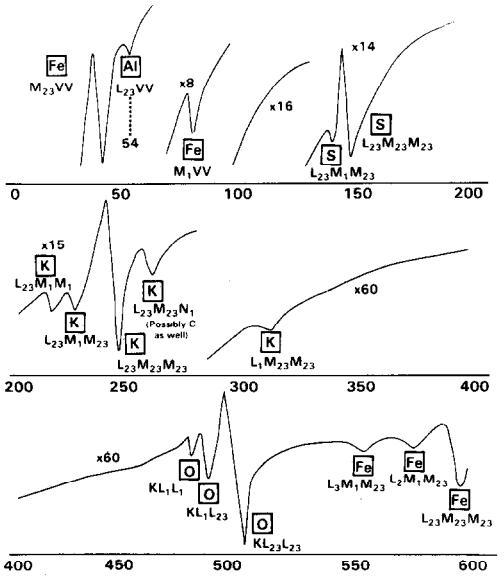

FIG. 1. AES spectrum (second derivative mode) of a completely reduced sample of the doubly promoted iron catalyst. Scale in electron volts.

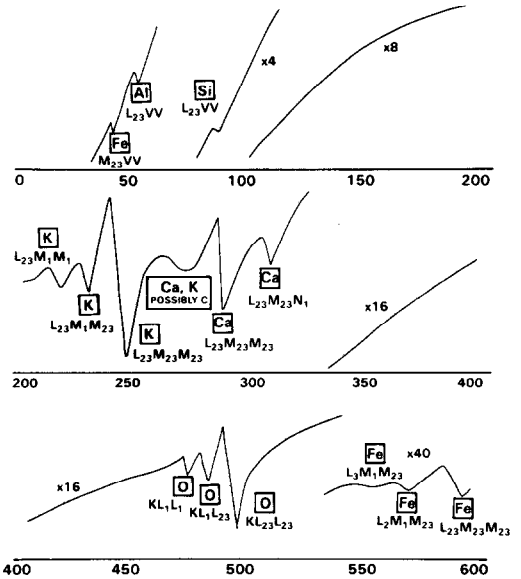

FIG. 3. AES spectrum (second derivative mode) of a completely reduced multiply promoted iron catalyst. Scale in electron volts.

oxygen in Al_2O_3 has also emerged (*19*). A multiply promoted catalyst that was treated in a similar manner showed only bulk metallic iron when observed by Mössbauer spectroscopy. Thus, the iron catalyst can definitely be assumed to be fully reduced. Some of the sulfur seen in Figs. 2 and 3 was present before the bakeout but after the initial reduction. The origin of the sulfur, sample vs chamber contamination, is unclear. Also, a potassium transition coincides with the carbon 272-eV transition. A small amount of carbon could have gone undetected.

Quantitative AES

To obtain quantitative surface analysis with AES, one must use the largest peaks and those peaks whose energies correspond to Auger electrons that originate near the surface, i.e., 40 to 600 eV. For this analysis, the 47-eV iron peak, the 54-eV aluminum (Al_2O_3) peak, the 149-eV sulfur peak, the 249-eV potassium peak, and the 508-eV oxygen peak were used. The aim is to obtain the surface composition without calibration of these peaks against a standard.

The Auger current is a function of a number of variables (*11, 13*). Such a functionality (following Chang (*11*)) can be represented as

$$I_{ij} = f(I_p, R, T, B, \psi_{ij}, \Phi_{ij}, D_{ij}, N_j). \quad (1)$$

All symbols are defined in the Appendix.

Many of the physical quantities on the right-hand side appear in the form of a product in their relationship to the Auger current. Meyer and Vrakking (*20*) have simply assumed that I_{ij} was proportional to the product of all quantities on the right-hand side of (1) except R as they were dealing with a smooth sample. They obtained reasonable values for some of the physical parameters when doing so. Fortunately, in the present problem, all quantities except the escape depth, D_{ij}, and the ionization cross section, Φ_{ij}, could be eliminated.

The roughness factor, R, the instrument transmission, T, and the primary current, I_p, are constant for all elements on the same sample. The backscattering factor, B, is important because it measures the enhancement of the Auger current of a given transition caused by backscattered primary and secondary electrons from within the sample. It involves the energy distribution of backscattered electrons in the sample, their angle with respect to the surface, and the ionization cross section of the surface elements ionized as a function of the electron energy. For iron catalysts, the secondary electron distribution is constant because these electrons are basically arising from a piece of metallic iron. The only entity affecting the enhancement to the Auger current is any difference in the functionality of the ionization cross section for each surface component with respect to the energy distribution. For all surface components on the catalyst and for low-energy primary beams, this factor has values of about 1.30 $\pm$ 0.15 (*20, 21*). Since few data exist for backscattering factors for surface species on a range of materials, this quantity is assumed to be a constant for all elements in the surface region.

The Auger transition probability, ψ_{ij}, is the probability that once an initial ionization occurs, then transition i follows. This probability accounts for two additional phenomena. The first one is the possibility that the atomic relaxation will occur through a process involving fluorescence. The probability of a fluorescent transition for the initial ionizations considered here is small, only about 1 to 2% (*22, 23*), and can be ignored.

Second, ψ_{ij} takes account of the probability that Coster–Kronig transitions from higher-energy initial ionizations within a subshell can enhance the Auger current of the lower-energy transition within the same subshell (*23*). This Coster–Kronig enhancement cannot be determined a *priori*. There has been little experimental work on this contribution for lower-atomic-number ele-

ments. Tracy has shown that an $L_1L_{23}V$ Coster–Kronig transition enhances the yield of the phosphorous $L_{23}VV$ transition of GaP when the primary electron beam is equal to or greater than the ionization energy of the L_1 shell (*24*). In an attempt to further delineate the role of these Coster–Kronig transitions, Ducharme and Gerlach (*25*) used a classical ionization cross section of the L_1 and L_{23} shells of chlorine and the M_1, M_{23}, and M_{45} shells of barium to show about a 20% enhancement to the measured L_{23} and M_{45} ionization cross sections when Coster–Kronig transitions are taken into account. They found that their experimentally measured ionization cross sections already corrected for Coster–Kronig enhancement. The ionization cross sections of the L_{23} and M_{23} shells used for the catalysts in this study were obtained by using data taken by them (*25, 26*). Coster–Kronig enhancement is partially accounted for in the measured or scaled values of Φ_{ij} for L and M shell transitions. Therefore, ψ_{ij} as a separate factor can be eliminated in this approach.

Equation (1) may now be simplified for the present analysis to

$$I_{ij} = f(\Phi_{ij}, D_{ij}, N_j). \tag{2}$$

A simple model can be used to relate the Auger current to the variables, ionization cross section, electron escape depth, and surface concentration.

In this simple model, the number of electrons that escape from the catalyst from depth z per unit time is related to the number of electrons that escape from the surface layer of atoms per unit time by means of an exponential decay, represented as

$$J_{z_{ij}} = J_{1_{ij}} e^{(-z/D_{ij})}. \tag{3}$$

The assumptions inherent in applying Eq. (3) to a physical system are discussed later.

The total current generated by this transition can be found by integrating from 0, the crystal surface, to ∞, far into the bulk. The resulting expression is

$$I_{ij} = \int_0^\infty J_{1_{ij}} e^{-(z/D_{ij})} dz \tag{4a}$$

or

$$I_{ij} = J_{1_{ij}} D_{ij}. \tag{4b}$$

Implicitly assumed is a microscopically smooth surface and an isotropic distribution of electrons that leave the surface. More importantly, this model assumes that the composition is constant with respect to depth. If the composition is a function of depth, an elemental distribution as a function of depth must be included in Eqs. (1) and (2). However, such information is usually not available, and this complication is ignored in this simple model. The limitation caused by this assumption is discussed later.

In order to compare the AES analysis, which samples a surface region, to the selective chemisorption analysis, which samples the surface, $J_{1_{ij}}$ is the desired quantity. However, I_{ij} is the measured quantity. Equation (4b) can be rearranged to

$$J_{1_{ij}} = I_{ij}/D_{ij} \tag{5}$$

and, in principle, the desired Auger current from the surface can be extracted from the measured Auger current from the surface region.

The current from the surface atoms of element j can be related to the concentration of element j on the surface through the ionization cross section. Once an initial vacancy occurs after ionization, there are a number of paths that the atom can follow in order to relax. These atomic relaxation paths are fluorescence and Auger transitions. Fluorescence is negligible. In addition, in this study, if more than one transition results from the same ionization event, the strongest transition is used. The current derived from these weaker transitions is assumed to be negligible. Therefore, if the initial electron vacancy distribution prior to any transition is assumed to be proportional to the ionization cross section (corrected

for Coster–Kronig enhancement (*25*)), then the Auger current can be assumed to be proportional to the ionization cross section. This assumption becomes less reliable, the greater the intensity of the ignored transitions that emanate from the common vacancy. Also, the Auger current from an element on the surface is proportional to the surface concentration of that element.

This discussion means that the Auger current from an element on the catalyst surface can be related to its concentration via

$$J_{1_{ij}} = k\Phi_{ij}N_j. \tag{6}$$

Therefore, by using Eq. (3) in (4) and rearranging

$$N_j = \frac{1}{k}(I_{ij}/\Phi_{ij}D_{ij}). \tag{7}$$

The total concentration of all elements then becomes

$$N_T = \sum_j N_j = \sum_j \frac{1}{k}(I_{ij}/\Phi_{ij}D_{ij}). \tag{8}$$

One transition, i, is used per element. The mole fraction of element j on the surface then becomes

$$X_j = \frac{N_j}{N_T} = \frac{I_{ij}/(\Phi_{ij}D_{ij})}{\sum_j (I_{ij}/(\Phi_{ij}D_{ij}))}. \tag{9}$$

If two or more elements are part of a compound, then the mole fraction of the compound can be estimated by using only one of its constituent elements in Eq. (9). In this case, I_{ij} for that element must be divided by the stoichiometric subscript of the element as it appears in the compound. On the surface, the element used must be unique to the compound. In this manner the surface promoter oxide mole fractions are obtained by using the Auger current from only the metal atoms in the promoters.

Equation (9) is the final result. The mole fraction of the surface species can be calculated from either known or reported parameters. No calibration is required. Assumptions inherent in Eq. (9) will be discussed later.

The Auger current, I_{ij}, was taken as the peak-to-peak height in the second derivative spectrum. Use of this measure of the Auger current would tend to underestimate the current. For modulation voltages that are small and for reasonably symmetrical peak shapes, the error is small (*21*). Since there were already approximations introduced in the analysis and some peaks were too small for a double integration with respect to energy, this procedure was judged to be unnecessary.

The ionization cross section, Φ_{ij}, either was taken directly from measurements of Gerlach and Ducharme (*27, 28*) or of Meyer and Vrakking (*19*) or was scaled via its near proportionality to the reciprocal of the square of the ionization energy for the same transition in adjacent elements. The iron M_{23} ionization cross section was calculated by assuming that it was an L_{23} ionization at the same energy as the M_{23} ionization. It was then scaled directly from the L_{23} data. A calculation based on the assumption that it was a K shell yielded a value for the M_{23} cross section that agreed with it within about 15%.

The escape depth corrects for the fact that electrons with higher kinetic energy have a higher probability of escaping from farther into the sample. It is a strong function of the electron kinetic energy. The values for D were taken from Tracy's escape depth curve as given by Chang (*12*). This curve agrees closely with values reported by Brundle (*29*). Tracy's curve is a smoothed-out compilation of escape depth data. Table 2 lists the element, transition, Φ_{ij}, and D_{ij} used in this work.

Surface Composition of Doubly Promoted Iron Catalyst

The data of Table 2 were used in Eq. (9) to obtain the results listed in Table 3 for the relative amount of each element on the surface of the doubly promoted iron catalyst.

If one assumes the following compounds, Al_2O_3 and K_2O, one obtains the surface composition outlined in Table 4 for the

TABLE 2

Values of the Ionization Cross Sections and Escape Depths for the Transitions Used in Determining Surface Composition by AES

Element	Transition (eV)	$\Phi(\times 10^{23})$ (m^2)	D (nm)
Oxygen	$KL_{23}L_{23}(508)$	1.3	1.00
Aluminum	$L_{23}V_0V_0(54)$	94.	0.45
Sulfur	$L_{23}M_{23}M_{23}(149)$	25.	0.55
Potassium	$L_{23}M_{23}M_{23}(249)$	5.8	0.65
Iron	$M_{23}VV(47)$	130.	0.45

TABLE 4

Surface Composition of Doubly Promoted Iron Catalyst by AES and Selective Chemisorption

Compound	Mole fraction by AES	Area fraction by sel. chem.	Area fraction by sel. chem. (*30*)
Fe	0.45	0.48	0.48
K_2O	0.43	0.37	0.38
Al_2O_3	0.03	0.15[a]	0.14[a]
S	0.09	—	—

[a] By difference.

doubly promoted catalyst. Included are the results of selective chemisorption. The oxygen AES signal is ignored in the calculation for Table 4 since it is accounted for by the metallic portion of the promoters.

This procedure was repeated for both the singly and multiply promoted iron catalysts. These results are shown in Tables 5 and 6.

DISCUSSION

Equation Limitations

One very important point is that the value calculated for X_j is completely dependent on the assumed model of the surface region. The X_j calculated by Eq. (3) implicitly assumes a uniform composition with respect to depth, at least to the maximum measurable escape depth for the electrons from the given transitions. If this criterion is not fulfilled, the elemental distribution in the surface region must be known before the values of X_j can be calculated properly. A surface structure cannot be inferred from AES alone.

A model will be presented later that indicates that the promoter is probably not uniformly distributed either across or through the surface region. Therefore, the assumption of a uniform surface region distribution implicit in Eq. (3) is not completely valid. A recalculation of the results with D_{ij} removed from Eq. (9) would give an indication of the effect of this parameter. Physically the elimination of the escape depth parameter implicitly assumes that all elements are present only to monolayer depth. Their electrons cannot have equal escape depths. The recalculations are shown in Table 7.

Though removal of the escape depth parameter has some effect on the results, the values shown in Table 7 are similar to

TABLE 3

Elemental Surface Composition as Determined by AES for the Doubly Promoted Iron Catalyst

Element	Number fraction
Iron	0.23
Potassium	0.42
Aluminum	0.03
Oxygen	0.27
Sulfur	0.05

TABLE 5

Surface Composition of Singly Promoted Iron Catalyst by Compound as Determined by the Al or O Auger Signal Compared to Selective Chemisorption

Compound	No. frac. based on Al signal	No. frac. based on O signal	Selective chemisorption (*5*)
Fe	0.71	0.58	0.45
Al_2O_3	0.21	0.35	0.55[a]
S	0.08	0.07	Undetected

[a] By difference.

TABLE 6

Surface Composition of Multiply Promoted Iron Catalyst as Determined by AES Compared to Selective Chemisorption (from Ref. (*31*))

Compound	Mole fraction by AES	Selective chemisorption
Fe	0.04	0.07
K_2O	0.41	0.59
CaO	0.50	
Al_2O_3	0.05	0.34[a]
SiO_2	Trace	

[a] By difference.

those in Tables 4 and 6. The reason is that the escape depth term ranges from 0.45 nm for iron to 0.65 nm for potassium, not a large difference. If oxygen, with an escape depth of about 1.0 nm, is included in the calculations, the effect of escape depth is more pronounced, as in the case of the singly promoted catalyst. Therefore, if the escape depths of the elements analyzed are similar, this parameter can be removed from Eq. (9).

TABLE 7

Recalculation of Surface Composition without Escape Depth Parameter

Catalyst	Component	Surface concentration
Doubly promoted	Fe	0.36
	K_2O	0.53
	Al_2O_3	0.02
	S	0.09
Multiply promoted	Fe	0.03
	K_2O	0.39
	CaO	0.55
	Al_2O_3	0.03
	SiO_2	Trace
Singly promoted		
Al based	Fe	0.70
	Al_2O_3	0.20
	S	0.10
O based	Fe	0.40
	Al_2O_3	0.54
	S	0.06

One other limitation must be placed on Eq. (9). Values of the ionization cross section must be available. These values must include the contribution of the backscattered electrons (if necessary) and the contribution of Coster–Kronig enhancement. At this time, the ionization cross section with inclusion of Coster–Kronig enhancement can be estimated for K, L_{23}, and some M_{23} initial ionizations (*21*). In order to study only the surface region (less than 1 nm or so), this limits the application of Eq. (9) to elements no heavier than those in about the first transition series in the periodic table.

Comparison of Selective Chemisorption vs AES

In view of the approximations introduced by the assumptions inherent in Eq. (9), its validity for quantitative analysis must first be shown. Through the comparison of the surface fractions of iron determined by both AES and the reliable technique of CO selective chemisorption, this validity can be established. The iron fractions of the surface reported in Tables 4 and 7 show good agreement between the two techniques, indicating that AES and Eq. (9) can be used quantitatively for these catalysts. Also, the K_2O surface composition determined by AES agrees with the value obtained by selective chemisorption of CO_2. By contrast, the Al_2O_3 concentration obtained by AES is significantly smaller than that obtained by difference of chemisorption and physisorption data.

The agreement between the K_2O surface compositions determined by AES and CO_2 selective chemisorption shown in Table 4 implies that CO_2 is selective for K_2O in the presence of Al_2O_3. However, since a K_2O–Al_2O_3 complex has been proposed (*1*) to explain the lack of decomposition of K_2O under reduction conditions, the small amount of Al_2O_3 determined by the aluminum peak in Table 4 was unexpected. There is no attenuation of this aluminum $L_{23}VV$ peak upon oxidation, even though

the transition shifts from 67 to 54 eV (*32*). The escape depth of the 54-eV Auger electrons is 0.4 to 0.5 nm. If this ion is somehow shielded from the surface by the potassium and/or oxygen ions, then fewer aluminum ions and hence less Al_2O_3 would be calculated than are actually present in the surface region (the depth of escape of Auger electrons). Therefore, this small amount of Al_2O_3 calculated could be a function of the location of this aluminum ion on the surface.

The AES-determined surface composition of the singly (Al_2O_3) promoted catalyst can only partially substantiate this argument because of the experimental procedure. A comparison of the results with and without the escape depth parameter included (Table 5 vs Table 7) indicates that the calculated surface concentration is dependent on the model chosen. However, by either calculation, the Al_2O_3 based on the AES oxygen signal is greater than that based on the aluminum signal. This observation does support the above hypothesis.

In addition, the Al 54-eV ($L_{23}VV$) peak emerged only after the singly and doubly promoted catalysts had completely reduced surfaces. This peak was absent when the surface was oxidized. The migration of Al_2O_3 to the surface of the catalyst during reduction appears to be consistent with previous findings. First, Maxwell *et al.* (*33*) examined the intensity of magnetization of unreduced and reduced iron catalysts. They found that in a singly promoted iron catalyst, some Al_2O_3 could be dissolved in the bulk in the unreduced state but none was in the iron phase in the reduced state. Later, Topsøe *et al.* (*34*) used Mössbauer spectroscopy to study the reduction of a singly (Al_2O_3) promoted iron catalyst. They concluded that the Al_2O_3 is present as inclusions of $FeAl_2O_4$ in an incompletely reduced catalyst but exists as a separate phase of Al_2O_3 inclusions ca. 2 nm in diameter in the reduced state. The present reduction results show that when the surface region is in the oxide state, no aluminum ion is detected. The Al_2O_3 could be dissolved in the surface region that was oxidized. However, more Al_2O_3 migrates to the surface as reduction proceeds until a final amount is reached. It is forced out of the iron lattice. In this same vein, sulfur is found on the surface only in the presence of reduced iron.

With the validity of Eq. (9) established as an estimation tool, a multiply promoted iron catalyst was examined. For this catalyst, CO_2 chemisorption is an ambiguous probe.

Once again, the iron concentrations determined by Eq. (9) and that reported elsewhere (*31*) are in substantial agreement. The equation is valid for over an order of magnitude change in surface iron concentration. In addition, the surface is composed predominantly of K_2O and CaO, though these components make up only a small percentage of the catalyst bulk. The Al_2O_3 fraction of this material is once again most likely in an orientation such that the Al^{3+} ion is shielded from the vacuum–solid interface.

MODEL OF SURFACE OF DOUBLY PROMOTED IRON CATALYST

From the AES and other results, a model of the surface of the doubly promoted iron catalyst can be proposed. The model is shown in Fig. 4. This model is consistent with all of the findings. The bulk of a singly promoted reduced iron crystallite has already been proposed to be composed of metallic iron with separate Al_2O_3 inclusions approximately 2 nm in diameter (*9*). This model is supported by X-ray examination, Mössbauer spectroscopy, and $H_2{}^{18}O$ exchange with the ^{16}O of the Al_2O_3 of the promoted iron catalysts (*4*, *34*, *35*). In the doubly promoted catalyst, these inclusions would tend to contain K_2O as well.

The K_2O–Al_2O_3 complex is believed to be present on the catalyst surface, and the K_2O is thus prevented from decomposing under reduction conditions. Its structure probably does not resemble that of $KAlO_2$

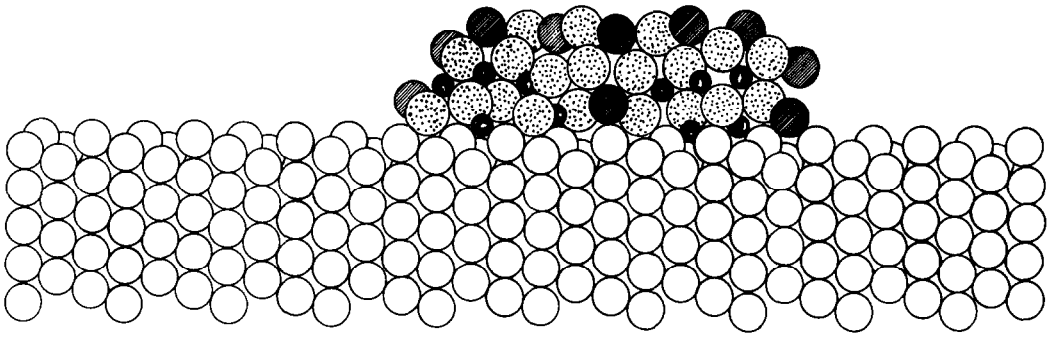

FIG. 4. Model of doubly (K_2O–Al_2O_3) promoted iron catalyst surface (○ = Fe; ◑ = Al; ● = K; ◌ = O).

but is fairly close packed instead. However, as in $KAlO_2$, the aluminum ions are most likely buried beneath the potassium and oxygen ions.

This structure is depicted in Fig. 4. The potassium and oxygen ions tend to be above the aluminum ions though some potassium ions probably lie within the island. Some could be in contact with iron atoms on the surface. The aluminum ions probably tend to occupy tetrahedral-type interstices between the oxygen ions, even though in pure γ-Al_2O_3 the aluminum ions occupy both tetrahedral and octahedral interstices. This complex would be on the surface as shown by the AES results. In fact, the island of promoter would probably be more likely to float above the iron surface than be buried within the surface region. There may be a small amount of penetration into the iron.

The island model means that these promoters are not believed to be mixed so that every promoter molecule has an adjacent iron atom and vice versa (*1*). This model is based on the following observations. The rate of ammonia synthesis at atmospheric pressure referred to unit iron surface area for the doubly promoted iron catalyst used here has been shown to be the same as that for large particles of iron supported on MgO (*36*). Also, this rate has been calculated to be the same for unpromoted and singly, doubly, and multiply promoted iron catalysts at atmospheric pressure (*37*). These findings support the idea of continuous areas of iron on the surface. Also, with the large amount of promoters observed, especially on the surface of multiply promoted catalysts, islands of promoter must be present, because there is not enough iron to completely surround each promoter molecule.

Therefore, the surface region is extremely nonuniform with promoter and iron both present in the region. These promoter islands are probably no more than 1.0 nm thick and are probably even thinner. This conclusion is supported by the fact that the 595-eV iron transition which arises from a depth of 1.2 to 1.4 nm changes by about a factor of 3 among singly, doubly, and multiply promoted catalysts, while the 47-eV peak changes by more than an order of magnitude. Obviously, iron below the promoter contributes significantly to the 595-eV Auger current.

APPENDIX: LIST OF SYMBOLS

- B = Backscattering coefficient (dimensionless)
- D = Escape depth of electrons (nm)
- I = Measured Auger current (C s^{-1})
- J_z = Auger current from element at atomic layer l (C nm^{-1} s^{-1})
- J_1 = Auger current from element on the surface (C nm^{-1} s^{-1})
- N = Surface concentration of element (mole m^{-2})

N_T = Surface concentration of all elements (mole m^{-2})
R = Roughness factor (dimensionless)
X = Mole fraction of element on surface
T = Instrument transmission
Φ = Ionization cross section (m^2)
ψ = Auger transition probability
k = Proportionality constant
z = Depth into bulk material (nm)

Subscripts

i = Transition
j = Element
z = Layer of atoms at depth z; at $z = 0$, l is defined as 1
p = Primary electrons

ACKNOWLEDGMENTS

We would like to thank Professor Paul Emmett for helpful discussions on the ammonia synthesis catalyst. This work was supported by National Science Foundation Grants NSF GK-17451X and NSF CPE 79-70156.

REFERENCES

1. Emmett, P. H., and Brunauer, S., *J. Amer. Chem. Soc.* **59,** 310 (1937).
2. Brunauer, S., and Emmett, P. H., *J. Amer. Chem. Soc.* **62,** 1732 (1940).
3. Brunauer, S., Emmett, P. H., and Teller, E., *J. Amer. Chem. Soc.* **60,** 309 (1938).
4. Solbakken, V., Solbakken, A., and Emmett, P. H., *J. Catal.* **15,** 90 (1969).
5. Westrik, R., and Zwietering, P., *Proc. K. Ned. Akad. Wet. Ser. B* **56,** 492 (1953).
6. Blyholder, G., and Neff, L. D., *J. Phys. Chem.* **66,** 1464 (1962).
7. Clarke, T. A., Gay, I. D., and Mason, R., *Surf. Sci.* **50,** 137 (1975).
8. Silverman, D. C., Ph.D. dissertation, Stanford University, 1975.
9. Van Cauivelaert, F. H., and Hall, W. K., *Trans. Faraday Soc.* **66,** 454 (1970).
10. Dry, M. E., du Plessis, J. A. K., and Leuteritz, B. M., *J. Catal.* **6,** 194 (1966).
11. Brennan, D., and Hayward, D. O., *Philos. Trans. R. Soc. London Ser. A* **258,** 375 (1965).
12. Chang, C. C., *in* "Characterization of Solid Surfaces" (P. F. Kane and G. B. Larrabee, Eds.), p. 307. Plenum, New York, 1974.
13. Fiermans, L., and Vennik, J., *in* "Advances in Electronics and Electron Physics" (L. Marton, Ed.), p. 139. Academic Press, New York, 1977.
14. Williams, F. L., and Boudart, M., *J. Catal.* **30,** 438 (1973).
15. Levy, R. B., and Boudart, M., *J. Catal.* **32,** 304 (1974).
16. Bokhoven, C., van Heerden, C., Westrik, R., and Zwietering, P., *in* "Catalysis" (P. H. Emmett, Ed.), Vol. III, Chap. 7, p. 283. Reinhold, New York, 1955.
17. Nielsen, A., "An Investigation on Promoted Iron Catalysts for the Synthesis of Ammonia," 3rd ed. Chap. 6, p. 142. Jul. Gjellerups Forlag, Copenhagen, 1968.
18. Hall, W. K., Tarn, W. H., and Anderson, R. B., *J. Amer. Chem. Soc.* **72,** 5436 (1950).
19. Quinto, D. T., and Robertson, W. D., *Surf. Sci.* **27,** 645 (1971).
20. Meyer, F., and Vrakking, J. J., *Surf. Sci.* **33,** 271 (1972).
21. Vrakking, J. J., and Meyer, F., *Surf. Sci.* **47,** 50 (1975).
22. Burhop, E. H. S., "The Auger Effect and Other Radiationless Transitions." Cambridge Univ. Press, Cambridge, 1952.
23. Sevier, K. D., "Low Energy Electron Spectrometry," Chap. 2. Wiley–Interscience, New York, 1972.
24. Tracy, J. C., *Surf. Sci.* **38,** 625 (1973).
25. Ducharme, A. R., and Gerlach, R. L., *J. Vac. Sci. Technol.* **11,** 281 (1974).
26. Grant, J. T., Haas, T. W., and Houston, J. E., *Surf. Sci.* **42,** 1 (1974).
27. Gerlach, R. L., and Ducharme, A. R., *Surf. Sci.* **32,** 329 (1971).
28. Ducharme, A. R., and Gerlach, R. L., *J. Vac. Sci. Technol.* **10,** 188 (1973).
29. Brundle, C. R., *Surf. Sci.* **48,** 99 (1975).
30. Bokhoven, C., van Heerden, C., Westrik, R., and Zwietering, P., *in* "Catalysis" (P. H. Emmett, Ed.), Chap. 7. Reinhold, New York, 1955.
31. Nielsen, A., and Bohlbro, H., *J. Amer. Chem. Soc.* **74,** 953 (1952).
32. Suleman, M., and Pattinson, E. B., *J. Phys. F* **1,** L21 (1971).
33. Maxwell, L. R., Smart, J. S., and Brunauer, S., *J. Chem. Phys.* **19,** 303 (1951).
34. Topsøe, H., Dumesic, J. A., and Boudart, M., *J. Catal.* **28,** 477 (1973).
35. Nielsen, A., "An Investigation on Promoted Iron Catalysts for the Synthesis of Ammonia," 3rd ed., 180ff. Jul. Gjellerups Forlag, Copenhagen, 1968.
36. Dumesic, J. A., Topsøe, H., Khammouma, S., and Boudart, M., *J. Catal.* **37,** 503 (1975).
37. Khammouma, S., Ph.D. dissertation, Standard University, 1972.